Journal of Endocrinological Investigation (2021) 44:1175–1184
https://doi.org/10.1007/s40618-020-01401-7

ORIGINAL ARTICLE

MiR-21-5p in macrophage-derived extracellular vesicles affects podocyte pyroptosis in diabetic nephropathy by regulating A20

X. Ding[1] · N. Jing[1] · A. Shen[1] · F. Guo[1] · Y. Song[1] · M. Pan[1] · X. Ma[1] · L. Zhao[1] · H. Zhang[1] · L. Wu[1] · G. Qin[1] · Y. Zhao[1]

Received: 19 March 2020 / Accepted: 19 August 2020 / Published online: 15 September 2020

Abstract

Objectives Podocyte pyroptosis, characterized by inflammasome activation, plays an important role in inflammation-mediated diabetic nephropathy (DN). Our study aimed to investigate whether miR-21-5p in macrophage-derived extracellular vesicles (EVs) could affect podocyte injury in DN.

Methods EVs were extracted after the treatment of RAW 264.7 (mouse macrophage line) with high glucose (HG). The podocyte pyroptosis was determined using the flow cytometry and the western blot. After the knockdown of miR-21-5p in HG-induced RAW264.7 cells, we injected the extracted EVs into DN model mice.

Results The level of miR-21-5p was higher in HG-stimulated macrophage-derived EVs than in normal glucose-cultured macrophage-derived EVs. The co-culture of EVs and podocytes promoted reactive oxygen species (ROS) production and activation of inflammatory in MPC5 cells (mouse podocyte line). However, restraint of miR-21-5p in EVs reduced ROS production and inhibit inflammasome activation in MPC5 cells, thereby reducing podocytes injury. Meanwhile, we found that miR-21-5p inhibited the A20 expression through binding with its 3′-untranslated regions in MPC5 cells. Further studies showed that A20 was also involved in the regulation of miR-21-5p of RAW 264.7-derived EVs on MPC5 injury. At the same time, it was also proved in the DN model mice that miR-21-5p in macrophage-derived EVs could regulate podocyte injury.

Conclusion MiR-21-5p in macrophage-derived EVs can regulate pyroptosis-mediated podocyte injury by A20 in DN.

Keywords Diabetic nephropathy · Extracellular vesicles · Podocyte · Macrophage · miR-21-5p · A20

Introduction

The incidence of diabetes has gradually elevated in recent years, and 40% of diabetic patients may have microvascular complications, namely diabetic nephropathy (DN), which is one of the most serious consequences of diabetes [1]. DN is the most common cause of end-stage renal disease, which is associated with a significantly elevated risk of cardiovascular disease and premature death [2]. The inflammatory response plays a central role in the progression of DN, and podocytes injury, which is the initial hallmark of DN plays an important role in inflammation-mediated DN [3, 4]. Classical activation of macrophages has pro-inflammatory effects and is a key process to aggravate renal damage [5]. It has been proven that macrophage-derived EVs can affect a variety of inflammatory diseases in animal inflammation models [6, 7].

Pyroptosis, a newly discovered programmed cell death, is characterized by inflammasome activation and activation of the cysteinyl aspartate-specific proteinase-1 (caspases-1) [8]. NLRP3 (nucleotide-binding domain, leucine-rich-containing family, pyrin domain-containing-3) is the most well-studied inflammasome, which is a multi-protein complex composed of NLR, ASC and caspase-l [9]. NLRP3 is responsible for activating caspase-1, thereby activating interleukin-1β (IL-1β) and interleukin-18 (IL-18) [10]. Bai M et al. demonstrated that NLRP3 inflammasome activation plays an important role in podocyte injury [11]. A20 is the protein encoded by the TNFAIP3 (tumor necrosis factor alpha-induced protein 3) gene as a central regulator of inflammatory signaling. Its main function is to protect tissue cells

Xiaoxu Ding and Na Jing contributed equally to this work and should be regarded as co-first authors.

✉ Y. Zhao
fcczhaoyy1@zzu.edu.cn

[1] Department of Endocrinology and Metabolism, The First Affiliated Hospital of Zhengzhou University, No. 1 Jianshe East Road, Zhengzhou City 450052, Henan, People's Republic of China

from injury via restraining the nuclear factor kappaB (NF-κB) transcription factor in the tumor necrosis factor-receptor (TNFR) and toll-like receptor (TLR) pathways, thereby playing an anti-inflammatory role in protecting tissue cells from damage [12, 13]. A20 is necessary to protect against kidney-related inflammation [14]. Studies found that A20 relieves inflammation by inhibiting NLRP3. A20/NLRP3 signaling axis is expected to be a potential therapeutic target for inflammation-related diseases, but whether A20/NLRP3 is involved in the development of DN needs further study.

EVs are a heterogeneous group of cell-derived membranous structures with diameters ranging from 40 to 1000 nm, mainly including exosomes and microvesicles [15]. Nevertheless, the purification of exosomes and microvesicles is still controversial [16]. EVs carry substances such as RNA, proteins, lipids, and DNA that can be absorbed by other cells and cause various phenotypic reactions [17]. Furthermore, studies have shown that miRNAs delivered through EVs can target mRNA levels after entering recipient cells [17–20]. The expression of miR-21-5p in the kidney is associated with renal survival, and abnormal expression in DN [21, 22]. Meanwhile, miR-21-5p in macrophage-derived EVs is associated with multiple diseases. For instance, miR-21-5p in macrophage-derived EVs induce Treg/Th17 cell imbalance to facilitate the development of epithelial ovarian cancer [23]; miR-21-5p in M2 macrophage-derived EVs regulates migration and invasion of colorectal cancer cells [24]. However, it is not clear whether miR-21-5p in macrophage-derived EVs is involved in DN. Our study aimed to investigate whether miR-21-5p in macrophage-derived EVs could affect the pyroptosis of podocytes.

Materials and methods

Cell culture

Mouse RAW 264.7 macrophages and MPC5 podocytes were purchased from the Cell Resource Center, Shanghai Institutes for Biological Sciences. The cells were cultured in Dulbecco's modified Eagle's medium/F12 supplemented (Gibco, Grand Island, New York, USA) with 10% fetal bovine serum (Biological Industries, Israel) and 1% penicillin/streptomycin 100X (Solarbio, Beijing, China) at 37 °C in 5% CO_2.

Isolation and characterization of EVs RAW 264.7 cells were cultured for 48 h. The dead cells and cellular debris were removed through centrifugation (800×*g* for 8 min). RAW 264.7 cells were filtered using a 0.2 mm filter. The filtered medium was centrifuged via ultracentrifugation (100,000×*g* for 5 h at 4 °C). After adding 1 × PBS, ultracentrifugation was performed at 100,000×*g* for 15 min. The pelleted EVs were resuspended in PBS and used immediately. The EVs were authenticated via electron microscopy and Western blot.

Animal studies

Male C57BL/6 mice (8–10 weeks old) were purchased from the experimental animal center of The First Affiliated Hospital of Zhengzhou University and fed under standard conditions. Mice weighing 20–30 g were selected for the experiment. Mice were fasted for 4 h and were intraperitoneally injected 50 mg/kg/day of streptozotocin (Sigma-Aldrich, St. Louis, MI, USA) in sodium citrate buffer (100 mmol/L, pH 4.5) or sodium citrate buffer (control), 5 straight days ($n = 6$). Glucose levels were measured from tail blood after 3 days. Mice with continuous 2 days of blood glucose above 16.4 mmol/L on continuous 3 days measurements were used in follow-up experiments. RAW 264.7 cells were stimulated with high glucose (25 mM) and transfected with miR-21-5p inhibitor or control. EVs were extracted from RAW 264.7 cells after 48 h and injected intravenously into mice four times (once every 2 weeks). The mice were sacrificed 8 weeks later, and the initial judgment of nephropathy (urine protein ≥ 30 mg/24 h) was performed according to changes in urine protein before sacrifice. All experiments were approved by the Animal Experimentation Ethics Committee of The First Affiliated Hospital of Zhengzhou University.

Quantitative real-time PCR (qRT-PCR)

The total RNA of cells or tissues was extracted using RNAsimple Total RNA Extraction Kit (Tiangen, Beijing, China). Then, the reverse-transcribed was executed via Mir-X™ miRNA First-Strand Synthesis Kit (TaKaRa, Dalian, China). QRT-PCR was performed on the ABI 7500 Real-Time PCR system (Applied Biosystems, Carlsbad, CA, USA) using SYBR Premix Ex Taq (TaKaRa). The relative expressions of miRNAs were normalized to U6, and calculated by the $2^{-\Delta\Delta Ct}$ method. The primers used are as follows: miR-21-5p: TGCGC TAGCT TATCA GACTG AT (forward), CCAGT GCAGG GTCCG AGGTA TT (reverse); U6: GCGCG TCGTG AAGCG TTC (forward), GTGCA GGGTC CGAGG T (reverse).

Western blotting (WB)

Cells or tissues were lysed using RIPA lysis buffer (Beyotime, Shanghai, China) and the lysates were detected via BCA kit (Beyotime). The proteins were denatured and separated through SDS-PAGE. The proteins were transferred onto PVDF membranes (Millipore, Billerica, MA, USA). The PVDF membrane was blocked for 2 h at 4 °C (Beyotime) and then incubated overnight with anti-Nephrin

antibody (ab216341; Abcam, Cambridge, UK), anti-podocin antibody (ab50339; Abcam), anti-NLRP3 antibody (ab263899; Abcam), anti-Caspase-1 antibody (ab138483; Abcam); anti-IL-1β antibody (ab205924; Abcam), anti-A20 antibody (ab92324; Abcam) or anti-β-actin antibody (ab6276; Abcam). The membrane was washed with TBST and incubated with the secondary antibody for 3 h at 4 °C. Detection was performed using the electrochemiluminescence (ECL) system (Beyotime). The β-actin was used as a control.

The detection of ROS

The cells were treated with 1 μmol/L DHR123 (Sigma-Aldrich) and incubated at room temperature in dark for 4 h. The cells were washed with PBS and were resuspended. The fluorescence intensity was detected by flow cytometry.

Cell transfection and treatment

MiR-21-5p inhibitor, inhibitor NC, si-A20 and si-NC were synthesized by Ribobio (Guangzhou, China); miR-21-5p mimic and mimic NC were synthesized by GenePharma (Shanghai, China). Lipofectamine 3000 (Invitrogen, Carlsbad, CA, USA) was used to transfect the cells. After transfection, cells were treated with 5.5 mmol/L glucose as the normal glucose group (NG; control), or 25 mmol/L glucose as high glucose group (HG), and cells were collected for subsequent detection after 48 h.

NG-M-EVs or the HG-M-EVs treated MPC5 cells. After treating HG or NG RAW 264.7 cells for 48 h, EVs were isolated from the supernatant and named the NG-M-EVs or the HG-M-EVs. Then, NG-M-EVs or the HG-M-EVs (25 μg/mL) was added to the MPC5 cell culture medium, and MPC5 cells were collected 48 h later.

Luciferase reporter assay

The interaction between miR-21-5p and A20 was explored via the dual luciferase reporter assay. The sequence of A20 3′ untranslated region (3′-UTR) containing the predicted miR-21-5p binding site was cloned into pmirGLO vector (Promega, Madison, WI, USA) as the wild-type (WT) A20 reporter vector. To construct mutant vectors, predicted miR-21-5p binding sites in A20 3′-UTR (Fig. 3F) were mutated using Quick Change Site-Direct Mutagenesis Kit (Stratagene, La Jolla, CA, USA). Mutated-type (Mut) A20 reporter vector as a negative control. MPC5 cells were co-transfected with the 3′-UTR of A20 (WT or Mut) luciferase reporter and miR-21-5p mimic or mimic NC via Lipofectamine 3000 (Invitrogen). After transfection for 48 h, luciferase assay kit (Promega) was used to detect luciferase activities. The relative luciferase activity of the miR-21-5p mimic group and the mimic NC group was detected.

Immunocytochemistry

The slides were hydrated with gradient alcohol and washed three times with distilled water. Antigen retrieval was carried out via treating the slide in citrate buffer for 12 min in the microwave. The slides were incubated with anti-podocin antibody (ab50339, Abcam) or anti-IL-1β antibody (ab205924; Abcam) at 4 °C overnight. After washing with PBS, tissues were treated with secondary antibodies for 50 min at 37 °C. After washing with PBS, tissues were treated in 0.5 g/L diaminobenzedine solution (Sigma-Aldrich) for 8 min, and were stained with hematoxylin for 3 min, rinsed, dehydrated, air dried and fixed. The results were observed under a microscope.

Statistical analysis

Results are expressed as mean ± SEM. Statistical analyses were performed via SPSS. The differences between two groups was assessed using Student's *t* test (two-tailed). The difference among multiple groups was compared using the one-way analysis of variance (ANOVA) followed by the LSD post hoc test. p value < 0.05 was considered statistically significant.

Results

MiR-21-5p was observably elevated in macrophage-derived EVs after cells treated with HG

Mouse macrophage cell line RAW 264.7 was treated with 5.5 mmol/L glucose (NG: control) or 25 mmol/L glucose (HG) for 48 h, and EVs were isolated from the supernatant and divided into the NG-M-EVs group and the HG-M-EVs group. We found that EVs were observed in both groups via electron microscopy (Fig. 1a) [25]. Meanwhile, we found that compared with the positive control group, EVs markers CD63 and TSG101 proteins [26] were abundant in NG-M-EVs group or the HG-M-EVs group, but no endoplasmic reticulum protein calnexin through WB (Fig. 1b). These results indicated that the EVs extraction was successful and relatively free of contamination [25, 27].

M-EVsM-EVs Furthermore, we detected six miRNAs associated with podocyte injury in EVs. The results showed that miR-155, miR-29a, and miR-21-5p were markedly elevated in macrophage-secreted EVs in the HG-M-EVs group, compared with the NG-M-EVs group (Fig. 1c). We selected

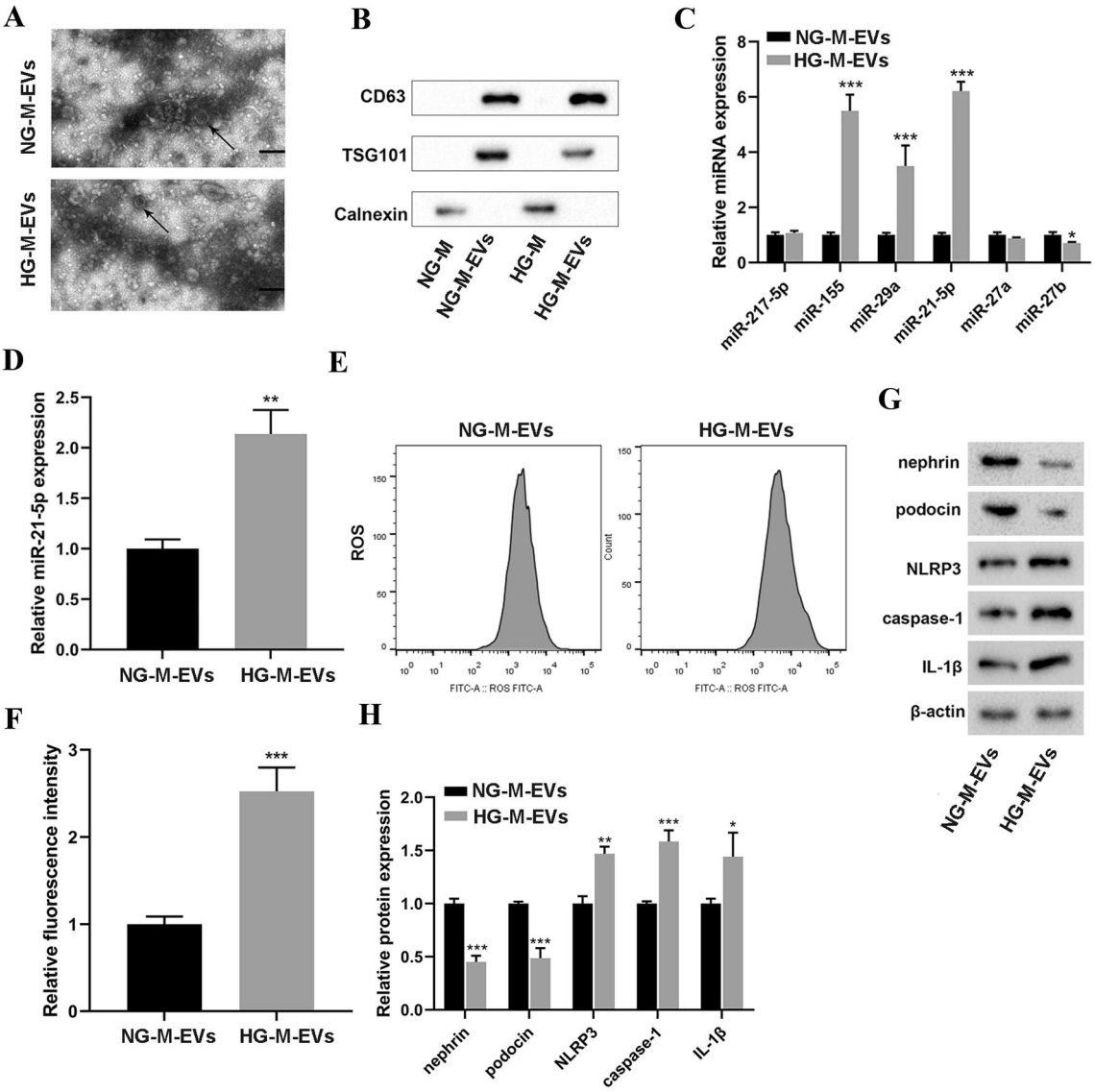

Fig. 1 Effect of HG-treated macrophage-derived EVs on podocyte injury. **a**–**c** The RAW264.7 (mouse macrophage line) cells were treated with 5.5 mmol/L glucose (normal glucose, NG) or 25 mmol/L glucose (high glucose, HG). After 48 h, EVs (M-EVs) were isolated from the supernatant and named the NG-M-EVs group or the HG-M-EVs group. $N=3$. **a** Identification of EVs by electron microscopy. **b** Cell lysates of RAW264.7 cells treated with NG or HG were used as positive controls (NG-M group or HG-M group). The protein levels of CD63, TSG101 and calnexin were detected in EVs via Western Blot. **c** Six miRNAs associated with podocyte injury were detected via qRT-PCR. **d**–**f** NG-M-EVs or the HG-M-EVs MPC5 (25 μg/mL) was added to the MPC5 cell culture medium, and MPC5 cells were collected 48 h later. $N=3$. **d** The expression of miR-21-5p was detected by qRT-PCR. **e**, **f** ROS content was measured via flow cytometry in cells, and fluorescence intensity reflects ROS content. **h, g** Podocyte markers nephrin and podocin proteins and inflammatory factors NLRP3, caspase-1, and IL-1β proteins were detected via Western blot. Data are presented as mean ± S.E.M. *P* values were analyzed by Student's *t* test. $N=3$. $^*P<0.05$, vs. NG-M-EVs

miR-21-5p with the most significant changes for follow-up studies.

Effect of HG-treated macrophage-derived EVs on podocyte injury

To explore the effects of HG-treated macrophage-derived EVs on podocytes pyroptosis, we treated MPC5 cells with HG-M-EVs or NG-M-EVs, respectively. We found that miR-21-5p was approximately 2.1-fold higher in podocytes treated with the HG-M-EVs group, compared with the NG-M-EVs group (Fig. 1d). To explore whether HG-treated macrophage-derived EVs affect the ROS production of podocytes, we examined ROS levels in two groups of podocytes and found that ROS was observably elevated in the HG-M-EVs group (Fig. 1e, f). At the same time, nephrin and

podocin proteins, which are expressed only in the podocytes in the kidney, are markedly lessened (Fig. 1g, h), further demonstrating the damage of podocytes [25, 28]. Inflammatory factors NLRP3, caspase-1, and IL-1β proteins were notably elevated in the HG-M-EVs group compared with the NG-M-EVs group (Fig. 1g, h). These results indicate that HG-treated macrophage-derived EVs are capable of inducing podocyte injury and activating inflammatory factors.

Effect of miR-21-5p in macrophage-derived EVs on podocyte injury

To explore whether miR-21-5p in macrophage-derived EVs affects podocytes, HG-treated RAW264.7 cells were transfected with miR-21-5p inhibitor or inhibitor NC (control), the EVs were then collected or co-cultured with MPC5 cells and named the miR-21-5p inhibitor-EVs group or the inhibitor NC-EVs group. The qR-PCR assay showed that miR-21-5p in the miR-21-5p inhibitor-EVs group was obviously reduced in EVs (Fig. 2a) and podocytes (Fig. 2b), compared with the inhibitor NC-EVs group. This indicated that miR-21-5p transfection was successful. Meanwhile, ROS levels of podocytes were obviously lessened in the miR-21-5p inhibitor-EVs group compared with the inhibitor NC-EVs group (Fig. 2c, d). Furthermore, nephrin and podocin proteins were markedly elevated in podocytes (Fig. 2e, f). It is further demonstrated that the podocyte injury was alleviated. We also found that NLRP3, caspase-1 and IL-1β proteins were notably elevated in the miR-21-5p inhibitor-EVs group compared with the inhibitor NC-EVs group (Fig. 2e, f). These results indicated that inhibition of miR-21-5p in

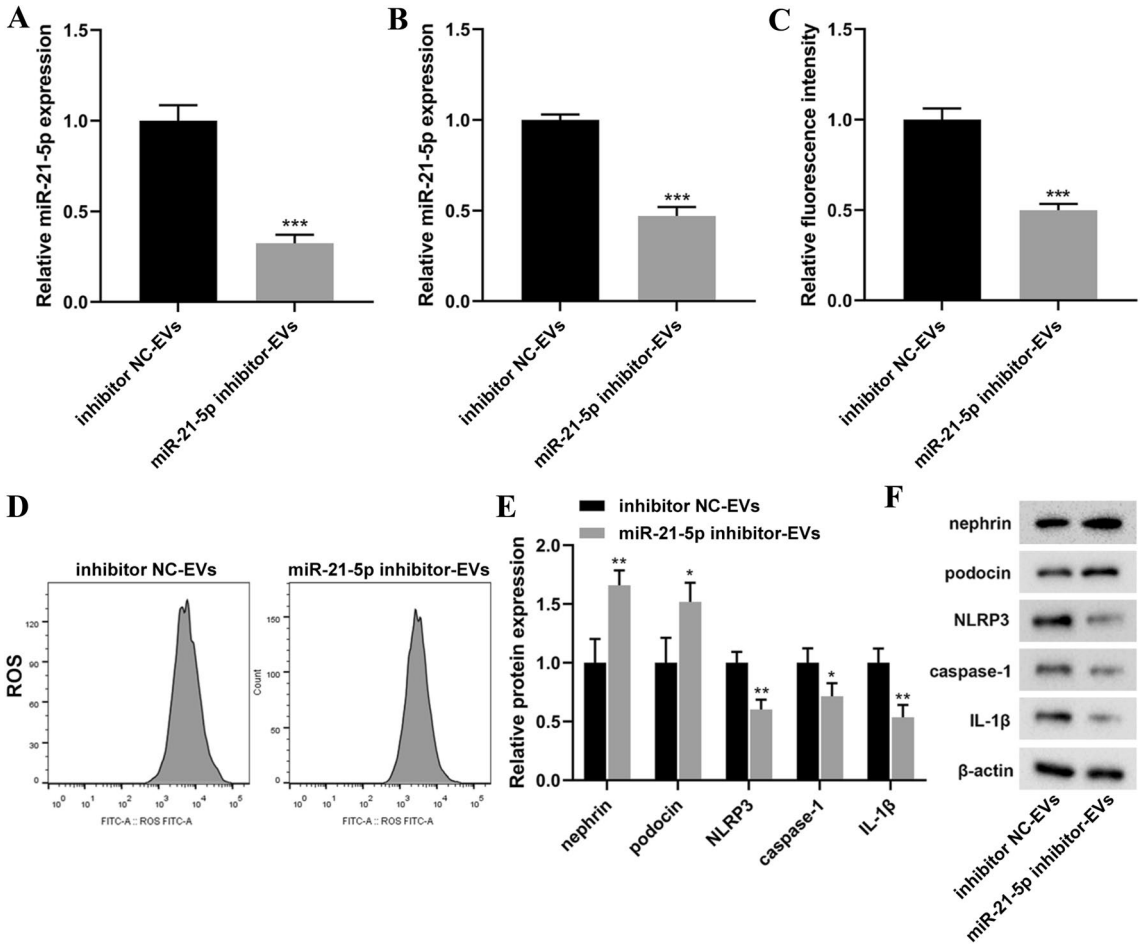

Fig. 2 Effect of miR-21-5p in macrophage-derived EVs on podocyte injury. **a**–**f** The RAW264.7 cells were transfected with miR-21-5p inhibitor or control (inhibitor NC) while treated with 25 mmol/L glucose for 48 h. The EVs in the supernatant were then collected and treated with (25 μg/mL) MPC5 cells 48 h, and named the inhibitor NC-EVs group or the miR-21-5p inhibitor-EVs group. $N=3$. **a** MiR-21-5p was detected in EVs via qRT-PCR. **b** MiR-21-5p was detected in MPC5 cells via qRT-PCR. **c**, **d** Flow cytometry was used to detect ROS content, and fluorescence intensity reflects ROS content. **e, f** Podocyte markers nephrin and podocin proteins and inflammatory factors NLRP3, caspase-1, and IL-1β proteins were detected via Western blot. Data are presented as mean ± S.E.M. *P* values were analyzed by Student's *t* test. $N=3$. $^*P<0.05$, vs. Inhibitor NC-EVs

HG-treated macrophages EVs could inhibit inflammatory and alleviate podocyte injury.

The potential mechanism of miR-21-5p affecting podocyte injury

To further verify the effect of miR-21-5p on podocyte injury, we overexpressed or knocked down miR-21-5p in MPC5 cells via transfection. Figure 3a indicates the successful transfection of miR-21-5p. The overexpression of

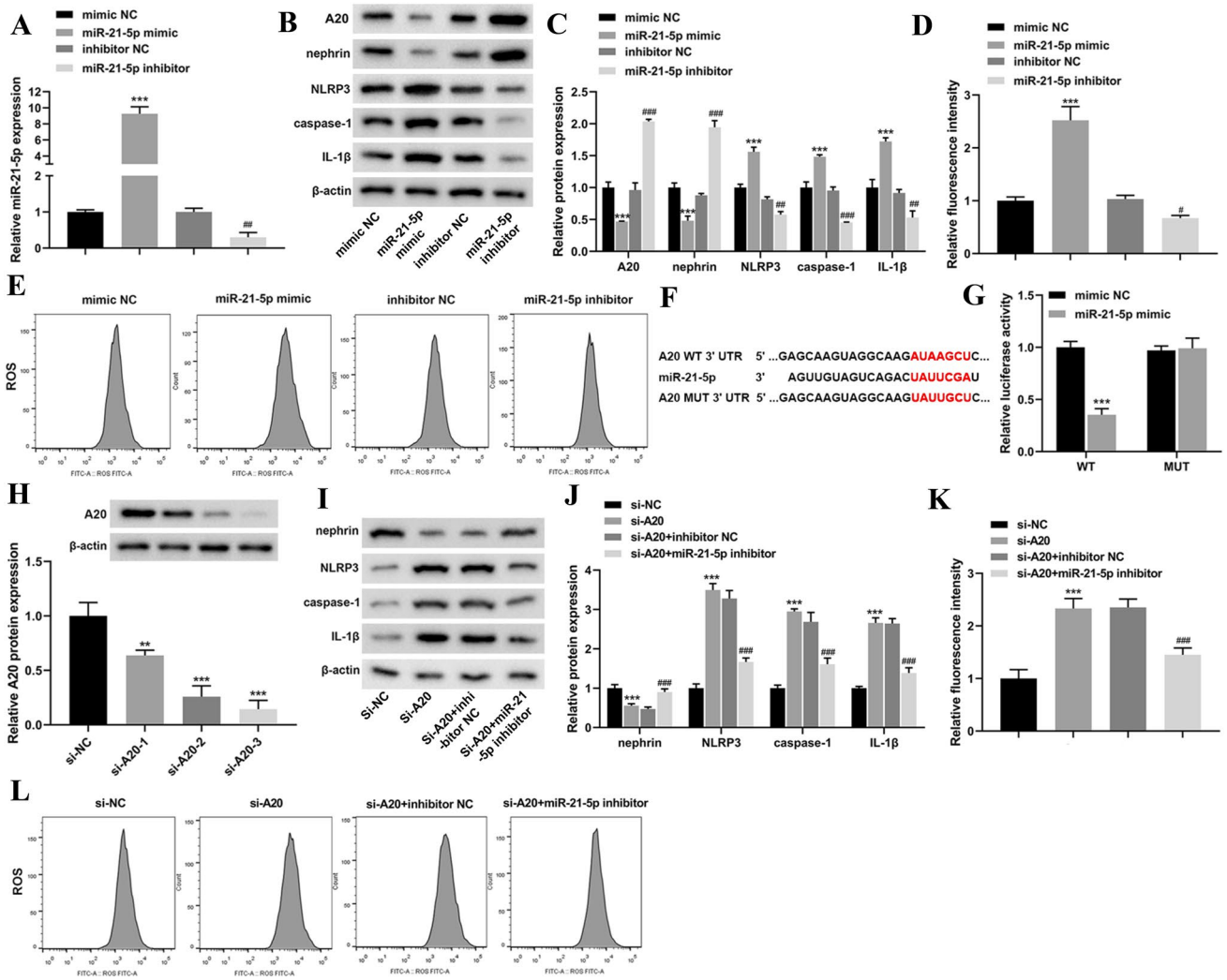

Fig. 3 The potential mechanism of miR-21-5p affecting podocyte injury. **a**–**e** MPC5 cells were transfected with miR-21-5p mimic, miR-21-5p inhibitor or corresponding control (NC), and divided into four groups: mimic NC, miR-21-5p mimic, inhibitor NC and miR-21-5p inhibitor. $N=3$. **a** The expression of miR-21-5p was detected through qRT-PCR. **b**, **c** The indexes of pod-cell damage and inflammation-related proteins were detected through Western blot. **d**, **e** Flow cytometry was used to detect ROS. **f**–**g** The potential binding sites of Mir-21-5p and A20 were predicted by bioinformatics software. A20 WT 3′-UTR is contained predicted miR-21-5p binding sites, A20 MUT 3′-UTR is the mutant predicted miR-21-5p binding site. MPC5 cells were co-transfected with the 3′-UTR of A20 (WT or Mut) luciferase reporter and miR-21-5p mimic or mimic NC. Then, dual-luciferase assay was performed. $N=3$. **h** MPC5 cells were treated with three si-A20s, and A20 expression was detected via qRT-PCR and western blot. $N=3$. After that, si-A20-3 with the highest transfection efficiency was selected for the follow-up study. **i**–**l** MPC5 cells were transfected or cotransfected with si-A20, miR-21-5p inhibitor or the corresponding controls (NC), and divided into four groups: si-NC, si-A20, si-A20 + inhibitor NC, si-A20 + miR-21-5p inhibitor. $N=3$. **i**, **j** Podocyte markers nephrin proteins and inflammatory factors NLRP3, caspase-1 and IL-1β proteins were detected via Western blot. **k**, **l** Flow cytometry was used to detect ROS, and fluorescence intensity reflects ROS content. Data are presented as mean ± S.E.M. P values were analyzed by Student's t test or ANOVA followed by the LSD post hoc test. $N=3$. $^{*}P<0.05$, vs. mimic NC or si-NC; $^{\#}P<0.05$, vs. Inhibitor NC or si-A20 + inhibitor NC

miR-21-5p in MPC5 cells significantly reduced the podocytes marker nephrin (Fig. 3b, c) and significantly elevated the ROS (Fig. 3 d, e). Meanwhile, we found that A20 protein was observably lessened but NLRP3, caspase-1, and IL-1β proteins were observably elevated (Fig. 3b, c). However, inhibition of miR-21-5p in MPC5 cells was contrary to the above. These results indicated that miR-21-5p can inhibit the expression of anti-inflammatory factor A20 and increase the expressions of inflammatory factors NLRP3, caspase-1 and IL-1β in podocyte, thereby affecting podocyte injury.

To investigate whether miR-21-5p would target A20 in podocytes, we predicted that the possible binding sites of miR-21-5p to 3′-UTR of A20 via software (Fig. 3f). Luciferase plasmids containing A20 3′-UTR with the predicted binding site of miR-21-5p (WT) or A20 3′-UTR with binding site mutation (MUT) were transfected into cells and transfected with miR-21-5p mimic or mimic NC. We performed the dual luciferase assay and found that the overexpression of miR-21-5p significantly reduced the activity of A20 WT, while the activity of A20 MUT was not affected. (Figure 3g). This suggests that A20 is a target of miR-21-5p. To explore whether miR-21-5p affects podocyte injury through regulating A20, we transfected or co-transfected si-A20-3 (Fig. 3h), miR-21-5p inhibitor, and control in MPC5 cells. We found that the nephrin protein was dramatically reduced after knockdown of A20 expression (Fig. 3i, j), and the ROS was obviously elevated in MPC5 cells (Fig. 3k, l), while the inflammatory factors NLRP3, caspase-1, and IL-1β were dramatically elevated (Fig. 3i, j). However, the inhibition of miR-21-5p reversed the results of the restraint of A20. These results indicate that miR-21-5p can target A20 to regulate inflammatory pathway-mediated podocyte injury.

MiR-21-5p in macrophage-derived EVs affects inflammatory pathway-mediated podocyte injury through A20

To explore whether miR-21-5p in macrophage-derived EVs could also affect A20-mediated inflammatory pathway-mediated podocyte injury, we stimulated RAW264.7 cells with HG while transfected miR-21-5p inhibitor or control, followed by the co-cultured with MPC5 cells transfected with si-A20 or control. In the miR-21-5p inhibitor-EVs group, we found that A20 and nephrin proteins were observably elevated; NLRP3, caspase-1, and IL-1β proteins were observably lessened (Fig. 4a, b); while ROS were obviously lessened in MPC5 cells (Fig. 4c, d), compared with the inhibitor NC-EVs group. Nevertheless, inhibiting A20 expression reversed the results via the miR-21-5p inhibitor in MPC5 cells (Fig. 4). These results indicated that miR-21-5p in macrophage-derived EVs can regulate inflammatory pathway-mediated podocyte injury through A20.

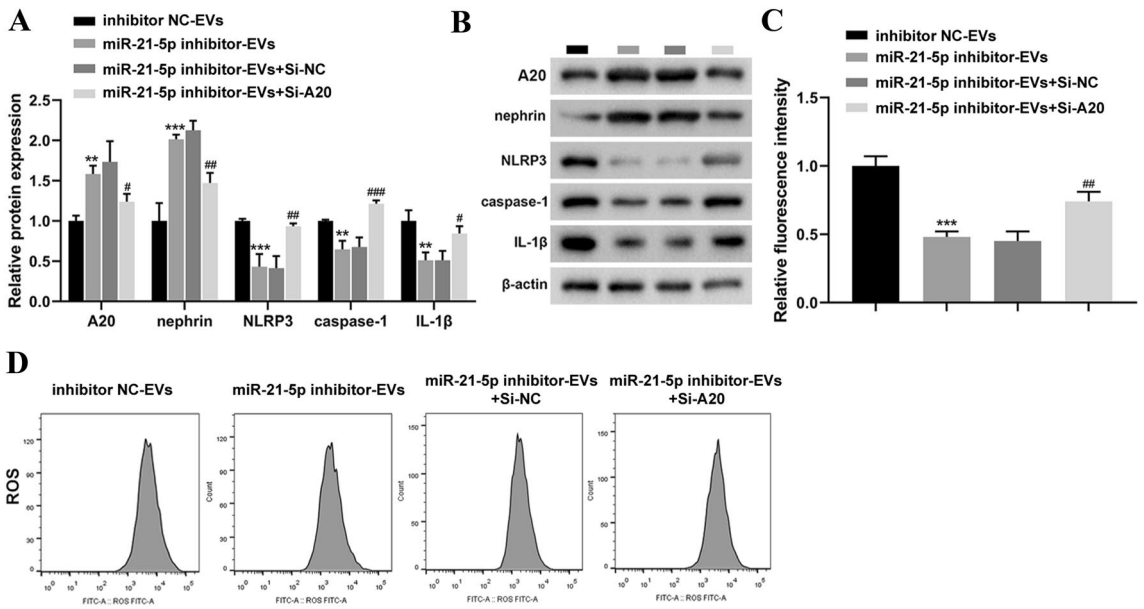

Fig. 4 MiR-21-5p in macrophage-derived EVs and A20 have an effect on podocytes injury. EVs of RAW264.7 cells were stimulated with 25 mmol/L glucose and transfected with miR-21-5p inhibitor (miR-21-5p inhibitor-EVs) or control (inhibitor NC-EVs) for 48 h, and co-cultured with MPC5 cells which transfected with si-A20 (miR-21-5p inhibitor-EVs + si-A20) or control (miR-21-5p inhibitor-EVs + si-NC) for 48 h. MPC5 cells were collected. $N = 3$. **a**, **b** A20, podocyte markers nephrin and inflammatory factors NLRP3, caspase-1 and IL-1β protein levels were detected via Western blot.**c**, **d** Flow cytometry was used to detect ROS levels, and fluorescence intensity reflects ROS content. Data are presented as mean ± S.E.M. *P* values were analyzed by ANOVA followed by the LSD post hoc test. $N = 3$. $^{*}P < 0.05$, vs. Inhibitor NC-EVs;$^{\#}P < 0.05$, vs. MiR-21-5p inhibitor-EVs + si-NC

To validate the above results in vivo, we extracted EVs from RAW264.7 cells, which were stimulated with HG and transfected with miR-21-5p inhibitor or control, and then injected intravenously into DN model mice [29]. In the M-EVs-miR-21-5p inhibitor group, the expression of miR-21-5p was obviously lessened in the kidney tissues, compared with the M-EVs-NC group (Fig. 5d). We detected levels of blood urea nitrogen (BUN) and serum creatinine (Scr) to evaluate renal function in the DN model mouse. In the M-EVs-miR-21-5p inhibitor group, we found BUN and Scr were markedly lessened compared with the M-EVs-NC group (Fig. 5a, b). Meanwhile, the level of podocyte marker podocin was increased and the level of IL-1β was decreased in M-EVs-miR-21-5p inhibitor group compared with M-EVs-NC by immunohistochemistry of renal tissues (Fig. 5c). These results revealed that the kidney injury in the M-EVs-miR-21-5p inhibitor group was reduced [30]. Furthermore, A20 protein expression was markedly elevated, and NLRP3, caspase-1, and IL-1β proteins were markedly lessened in the M-EVs-miR-21-5p inhibitor group (Fig. 5e, f). These results were consistent with the results of in vitro cell experiments, which further confirmed that miR-21-5p in macrophage-derived EVs could regulate inflammatory pathway-mediated podocyte injury through A20.

Discussion

Pyroptosis is primarily characterized by activating inflammasomes and accelerating the activation of the inflammatory signaling pathway [8]. Studies have shown that restraining inflammatory factors can curb pyroptosis and improve DN [31]. Therefore, restraint the pyroptosis of podocytes is salutary to develop new therapeutic DN strategies. There have been many studies demonstrating that miRNAs transferred via EVs are capable of targeting regulated mRNA levels upon entry into recipient cells, which affects a variety of diseases [17, 32]. However, whether miRNAs in macrophage-derived EVs are involved in podocyte pyroptosis has been rarely reported. Our study

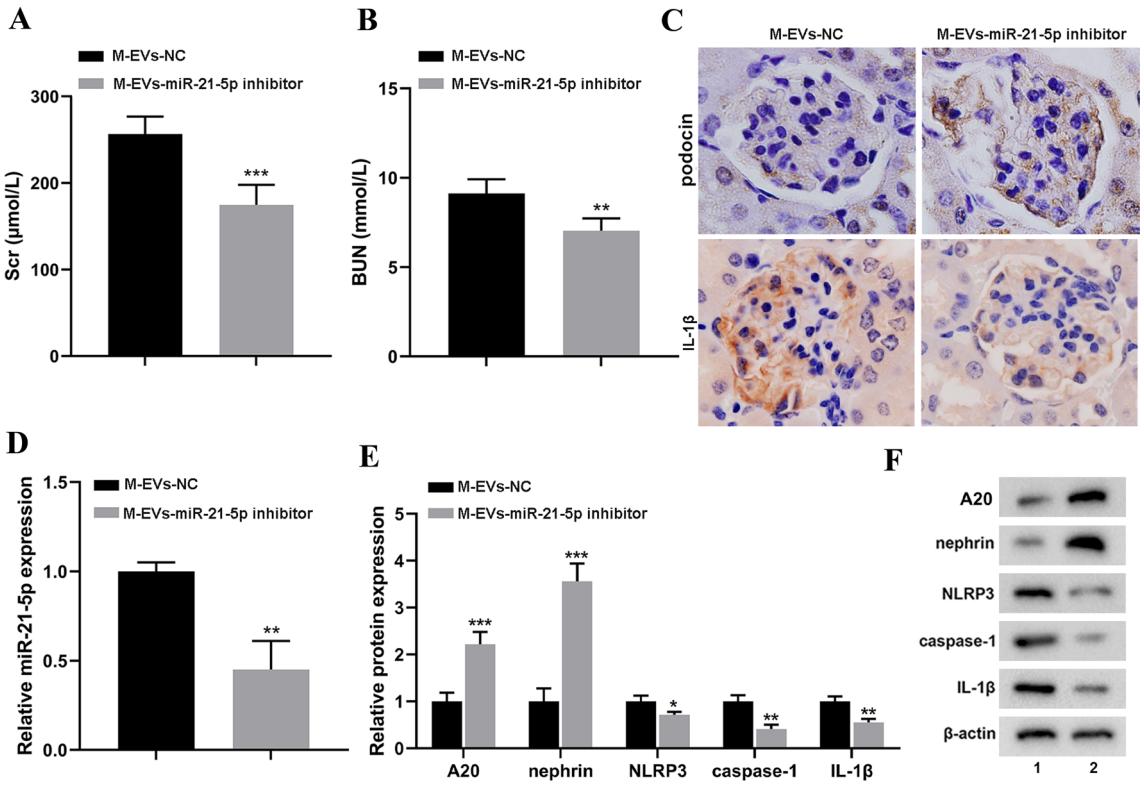

Fig. 5 MiR-21-5p in macrophage-derived EVs and A20 have an effect on renal injury. EVs of RAW264.7 cells stimulated with 25 mmol/L glucose and transfected with miR-21-5p inhibitor (M-EVs-miR-21-5p inhibitor) or control (M-EVs-NC) for 48 h. Then, EVs were collected and injected into STZ-induced DN model mice via the tail vein. The mice were sacrificed eight weeks later. $N=6$. **a**, **b** The levels of blood urea nitrogen (BUN) and serum creatinine (Scr) in peripheral blood were examined. **c** in the protein levels of podocyte marker Podocin and IL-1β were detected via immunohistochemistry in renal tissue. **d** MiR-21 expression in renal tissue was detected via qRT-PCR. **e, f** A20, podocyte markers nephrin and inflammatory factors NLRP3, caspase-1 and IL-1β protein levels were detected via Western blot (1 represents the M-EVs-NC group and 2 represents the M-EVs-miR-21-5p inhibitor group). Data are presented as mean ± S.E.M. P values were analyzed by Student's t test. $^*p<0.05$, vs. M-EVs-NC

demonstrated that miR-21-5p in macrophage-derived EVs could regulate podocyte pyroptosis through A20, providing a new therapeutic strategy for the treatment of DN.

Many studies revealed that miR-21-5p accelerates the development of inflammation [33]. Moreover, miR-21-5p in macrophage-derived EVs will also affect multiple diseases. For instance, miR-21-5p in macrophage-derived EVs directly targets Smad7, thereby accelerating fibrogenesis in tendon cells [34]. Our study found that the expression of miR-21-5p was observably elevated in macrophage-derived EVs with HG treatment. Furthermore, the reduction of miR-21-5p in macrophage-derived EVs reduces ROS levels and increases the protein levels of nephrin and podocin. Meanwhile, the protein levels of NLRP3, caspase-1, and IL-1β were decreased. Nephrin and podocin proteins are podocyte markers, which can be significantly reduced by podocyte damage [25, 28]. Studies have shown that ROS production is markedly elevated in HG-induced podocyte pyroptosis, and reducing ROS production can inhibit HG-induced podocyte pyroptosis [35]. Moreover, the ROS of mitochondria is a common mode of activation of NLRP3, and mito-tempo which is a mitochondrial ROS scavenger inhibits activation of NLRP3 [36]. Many studies have demonstrated that miR-21-5p accelerates the development of inflammation [37]. Moreover, miR-21-5p in macrophage-derived EVs also affects multiple diseases. For instance, miR-21-5p in macrophage-derived EVs directly targets Smad7, thereby accelerating fibrogenesis in tendon cells [34]. These results indicate that the reduction of miR-21-5p in macrophage-derived EVs can inhibit podocyte pyroptosis.

Studies revealed that knockdown of A20 promotes the inflammation and damages the central nervous system by activating NLRP3 in microglia (38). Our study also showed that restraint of A20 in podocytes notably increased NLRP3 and downstream caspases-1 and IL-1β. Further studies showed that miR-21-5p could target to inhibit A20 (Fig. 3). We speculated that miR-21-5p in macrophage-derived EVs may regulate pyroptosis of podocytes via targeting A20. Then, we proved this theory in cells by reversing the experiment (Fig. 4). We further confirmed in vivo that miR-21-5p in macrophage-derived EVs could regulate inflammatory pathway mediated podocyte injury through targeting A20 (Fig. 5).

In conclusion, our study found that miR-21-5p in macrophage-derived EVs through targeted inhibition of A20 can elevate the inflammasome NLRP3, caspases-1 and IL-1β related to pyroptosis, and augment the production of ROS, thereby causing podocyte injury. On account of podocyte injury plays an important role in inflammation-mediated DN [3, 4], miR-21-5p in macrophage-derived EVs is expected to be a new target for the treatment of DN.

Acknowledgements This work was supported by the National Natural Science Foundation of China (81800734).

Funding This work was supported by the National Natural Science Foundation of China (81800734).

Compliance with ethical standards

Conflict of interest The authors declare that there is no conflict of interest.

Research involving human participants and/or animals All experiments were approved by the Animal Experimentation Ethics Committee of The First Affiliated Hospital of Zhengzhou University.

Informed consent No informed consent.

References

1. Mcknight AJ, Duffy S, Maxwell AP (2015) Genetics of diabetic nephropathy: a long road of discovery. Curr Diabetes Rep 15:41
2. Flyvbjerg A (2017) The role of the complement system in diabetic nephropathy. Nat Rev Nephrol 13:311
3. Jun W, Hirofumi M (2013) Inflammation and the pathogenesis of diabetic nephropathy. Clin Sci 124:139–152
4. Maezawa Y, Takemoto M, Yokote K (2015) Cell biology of diabetic nephropathy: roles of endothelial cells, tubulointerstitial cells and podocytes. J Diabetes Investig 6:3
5. Zhao Y, Guo Y, Jiang Y, Zhu X, Liu Y, Zhang X (2017) Mitophagy regulates macrophage phenotype in diabetic nephropathy rats. Biochem Biophys Res Commun 494:42
6. Shenoda BB, Ajit SK (2016) Modulation of immune responses by exosomes derived from antigen-presenting cells. Clin Med Insights Pathol 9:1–8
7. Cypryk W, Nyman TA, Matikainen S (2018) From inflammasome to exosome-does extracellular vesicle secretion constitute an inflammasome-dependent immune response? Front Immunol 9:2188
8. Bergsbaken T, Fink S, Cookson B (2009) Pyroptosis: host cell death and inflammation. Nat Rev Microbiol 7:99–109
9. Olaf G, Thomas CJ, Greta G, Jurg T (2011) The inflammasome: an integrated view. Immunol Rev 243:136–151
10. Abderrazak A, Syrovets T, Couchie D, Hadri KE, Friguet B, Simmet T, Rouis M (2015) NLRP3 inflammasome: from a danger signal sensor to a regulatory node of oxidative stress and inflammatory diseases. Redox Biol 4:296–307
11. Bai M, Chen Y, Zhao M, Zhang Y, He JC, Huang S, Jia Z, Zhang A (2017) NLRP3 inflammasome activation contributes to aldosterone-induced podocyte injury. Am J Physiol Renal Physiol 312:F556–F564
12. Beatrice C, Isabelle C, Rudi B (2009) A20: central gatekeeper in inflammation and immunity. J Biol Chem 284:8217
13. Musone SL, Taylor KE, Lu TT, Joanne N, Ferreira RC, Ward O, Nataliya S, Petri MA, Ilyas KM, Susan M (2008) Multiple polymorphisms in the TNFAIP3 region are independently associated with systemic lupus erythematosus. Nat Genet 40:1062–1064
14. Kunter U, Daniel S, Arvelo MB, Choi J, Shukri T, Patel VI, Longo CR, Scali ST, Shrikhande G, Rocha E (2005) Combined expression of A1 and A20 achieves optimal protection of renal proximal tubular epithelial cells. Kidney Int 68:1520

15. van Niel G, D'Angelo G, Raposo G (2018) Shedding light on the cell biology of extracellular vesicles. Nat Rev Mol Cell Biol 19:213–228
16. Théry C, Witwer KW (2018) Minimal information for studies of extracellular vesicles 2018 (MISEV2018): a position statement of the International Society for Extracellular Vesicles and update of the MISEV2014 guidelines. J Extracell Vesicles 7:1. https://doi.org/10.1080/20013078.2018.1535750
17. O'Brien K, Breyne K, Ughetto S, Laurent LC (2020) RNA delivery by extracellular vesicles in mammalian cells and its applications. Nat Rev Mol Cell Biol. https://doi.org/10.1038/s41580-020-0251-y
18. Guduric-Fuchs J, O'Connor A, Camp B, O'Neill CL, Medina RJ, Simpson DA (2012) Selective extracellular vesicle-mediated export of an overlapping set of microRNAs from multiple cell types. BMC Genomics 13:357
19. Squadrito ML, Baer C, Burdet F, Maderna C, Gilfillan G, Lyle R, Ibberson M, Depalma M (2014) Endogenous RNAs modulate MicroRNA sorting to exosomes and transfer to acceptor cells. Cell Rep 8:1432–1446
20. O'Brien K, Breyne K, Ughetto S, Laurent LC (2020) RNA delivery by extracellular vesicles in mammalian cells and its applications. Nat Rev 1–22
21. Gholaminejad A, Tehrani HA, Fesharaki MG (2018) Identification of candidate microRNA biomarkers in diabetic nephropathy: a meta-analysis of profiling studies. J Nephrol 23:1–19
22. Hennino MF, Buob D, Van HC, Gnemmi V, Jomaa Z, Pottier N, Savary G, Drumez E, Noël C, Cauffiez C (2016) miR-21-5p renal expression is associated with fibrosis and renal survival in patients with IgA nephropathy. Sci Rep 6:27209
23. Zhou J, Li X, Wu X, Zhang T, Zhu Q, Wang X, Wang H, Wang K, Lin Y, Wang X (2018) Exosomes released from tumor-associated macrophages transfer miRNAs that induce a Treg/Th17 cell imbalance in epithelial ovarian cancer. Cancer Immunol Res 6(12):1578–1592
24. Lan J, Sun L, Xu F, Liu L, Hu F, Song D, Hou Z, Wu W, Luo X, Wang J (2019) M2 Macrophage-derived exosomes promote cell migration and invasion in colon cancer. Cancer Res 79(1):146–158
25. Lässer C, Alikhani VS, Ekström K, Eldh M, Paredes PT, Bossios A, Sjöstrand M, Gabrielsson S, Lötvall J, Valadi H (2011) Human saliva, plasma and breast milk exosomes contain RNA: uptake by macrophages. J Transl Med 9:9
26. Sun Z, Wang L, Dong L, Wang X (2018) Emerging role of exosome signalling in maintaining cancer stem cell dynamic equilibrium. J Cell Mol Med 22:3719–3728
27. Koh YQ, Almughlliq FB, Vaswani K, Peiris HN, Mitchell MD (2018) Exosome enrichment by ultracentrifugation and size exclusion chromatography. Front Biosci 23:865
28. Schell C, Huber TB (2017) The evolving complexity of the podocyte cytoskeleton. J Am Soc Nephrol 28:3166
29. Qi XM, Wang J, Xu XX, Li YY, Wu YG (2016) FK506 reduces albuminuria through improving podocyte nephrin and podocin expression in diabetic rats. Inflamm Res 65:103–114
30. Hu X, Zhang X, Jin G, Shi Z, Sun W, Chen F (2017) Geniposide reduces development of streptozotocin-induced diabetic nephropathy via regulating nuclear factor-kappa B signaling pathways. Fundam Clin Pharmacol 31:54–63
31. Li X, Zeng L, Cao C, Lu C, Lian W, Han J, Zhang X, Zhang J, Tang T, Li M (2017) Long noncoding RNA MALAT1 regulates renal tubular epithelial pyroptosis by modulated miR-23c targeting of ELAVL1 in diabetic nephropathy. Exp Cell Res 350:327–335
32. Kosaka N, Yoshioka Y, Fujita Y, Ochiya T (2016) Versatile roles of extracellular vesicles in cancer. J Clin Investig 126:1163–1172
33. Ge X, Huang S, Gao H, Han Z, Chen F, Zhang S, Wang Z, Kang C, Jiang R, Yue S (2016) miR-21-5p alleviates leakage of injured brain microvascular endothelial barrier in vitro through suppressing inflammation and apoptosis. Brain Res 1650:31–40
34. Cui H, He Y, Chen S, Zhang D, Yu Y, Fan C (2019) Macrophage-derived mirna-containing exosomes induce peritendinous fibrosis after tendon injury through the miR-21-5p/Smad7 pathway. Mol Ther Nucleic Acids 14:114–130
35. Toyonaga J, Tsuruya K, Ikeda H, Noguchi H, Yotsueda H, Fujisaki K, Hirakawa M, Taniguchi M, Masutani K, Iida M (2011) Spironolactone inhibits hyperglycemia-induced podocyte injury by attenuating ROS production. Nephrol Dial Transpl 26:2475–2484
36. Nakahira K, Haspel JA, Rathinam VA, Lee SJ, Dolinay T, Lam HC, Englert JA, Rabinovitch M, Cernadas M, Kim HP, Fitzgerald KA, Ryter SW, Choi AM (2011) Autophagy proteins regulate innate immune responses by inhibiting the release of mitochondrial DNA mediated by the NALP3 inflammasome. Nat Immunol 12:222–230
37. Voet S, Guire C, Hagemeyer N, Martens A, Schroeder A, Wieghofer P, Daems C, Staszewski O, Walle LV, Jordao MJC (2018) A20 critically controls microglia activation and inhibits inflammasome-dependent neuroinflammation. Nat Commun 9:2036